Article ID: 1003－6326(2003)04－0764－05

Primary crystallization process of rapidly solidified Al-Ni-Cu-Nd metallic glasses under continuous heating regime①

XIAO YU-de(肖于德)[1,2,3], LI Wen-xian(黎文献)[1], D. Jacovkis[2], N. Clavaguera[3], M. T. Clavaguera-Mora[2], J. Rodriguez-Viejo[2]

(1. School of Materials science and Engineering, Central South University, Changsha 410083, China;
2. Grup de Fisica de Materials I, Departament de Fisica, Universitat Autonoma de Barcelona, 08193 Bellaterra, Spain;
3. Fisica de l'Estat Solid, Facultat de Fisica, Universitat de Barcelona, Diagonal 647, 08028 Barcelona, Spain)

Abstract: Rapidly solidified $Al_{87}Ni_7Cu_3Nd_3$ metallic glasses were prepared by using melt spinning. Its calorimetric behavior was characterized by using differential scanning calorimeter. The metallic glasses were partially crystallized under continuous heating regime. Primary crystallization was studied through structural characterization of the amorphous and partially crystallized ribbons by means of conventional X-ray diffraction and transmission electron microscopy with selected area electron diffraction. The results show that, the as-spun ribbons are fully amorphous and homogeneous on the micron scale, but contain high density of nanoscale quenched-in clusters or crystallite embryos. Primary crystallization mainly leads to formation of two-phase mixture of α-Al nanocrystalline and residual amorphous phase. Precipitation of α-Al nanoparticles is limited by build-up and overlapped diffusion field of solute atoms with low diffusion rate. At the earlier stage of primary crystallization the crystal nuclei exhibit high density and growth rate. With the α-Al crystal growing, the crystal growth rate decreases, and even at the later stage further crystallization into α-Al crystal becomes difficult to occur due to thermal stabilization of the residual nickel and neodymium-enriched amorphous phase, the saturated values of crystallized volume fraction and α-Al crystal diameter getting to 20%－30% and 5－15 nm.

Key words: rapid solidification; Al-rich amorphous alloy; crystallization; nucleation; grain growth mechanism

CLC number: TG 146 **Document code:** A

1 INTRODUCTION

Many Al-based amorphous/nanocrystalline alloys containing transition metal (TM = Fe, Co, Ni, Cu, etc) and rare earth (RE = La, Y, Ce, Nd, etc) elements have an attractive combination of mechanical properties[1-3]. In the last ten years a wide interest was spurred to research primary crystallization of Al-rich metallic glasses[4-9].

The nanophase composites of Al-TM-RE system can be obtained by a suitable processing combination of rapid solidification and heat treatment[10-16]. As an important well-controlled method, annealing treatment based on primary crystallization was used widely to devitrify the Al-rich metallic glasses, to produce the novel nanophase composites consisting of the novel ultra fine microstructure with large quantity of α-Al nanoparticles embedded dispersively in an Al-rich amorphous matrix[17-23], and the optimum diameter and volume fraction of primary nanocrystalline particles are around 5－20 nm and 20%－30%, respectively[24]. However, many further studies ought to be done carefully in order to control effectively devitrification process to obtain an ideal nanoscale structure with optimized combination of mechanical properties.

In this work, our purpose is to examine nanostructural evolution during primary crystallizion in rapidly solidified Al-Ni-Cu-Nd metallic glass under continuous heating regime.

2 EXPERIMENTAL

The Al based metallic glass ribbons, less than 3 mm wide and 30 μm thick, were prepared by using a single copper roll melt-spinner. Chemical composition (mole fraction, %) of the ribbons was $Al_{87}Ni_7Cu_3Nd_3$[13-16].

Differential scanning calorimetric (DSC) curve of the as-quenched ribbons was obtained under continuous heating regime at 40 ℃/min in an Ar atmosphere by using a Perkin-Elmer DSC-7. The as-quenched specimens were crystallized partially through heating continuously up to various tempera-

① **Received date:** 2002－10－16; **Accepted date:** 2003－03－27

Correspondence: XIAO Yu-de, Associate professor, PhD; Tel: +86-731-8830261; E-mail: xiaoyude@mail.csu.edu.cn

tures between 90 ℃ and 310 ℃ at 40 ℃/min. The specimens were cooled at 160 ℃/min after thermal exposure.

X-ray diffraction (XRD) was used to identify phases existing in the as-spun and annealed ribbons and to measure the relative amount and mean diameter of primary crystallized particles in these ribbons. The XRD experiment was carried out in a SIEMENS D500 X-ray diffraction meter with a monochromatic Cu K_α (λ= 1.541 8 Å) radiation, scanning over a narrow range of scattering angle (2θ= 30°—50°) at a step of 0.03°.

The HRTEM foils were prepared by ion milling in a liquid nitrogen (N_2) bath, and examined in a CM30 high resolution transmission electron microscope at 300 kV, and the HRTEM images were analyzed using the digital micrograph software, and selected area electron diffraction (SAED) patterns by using the ProcessDiffration software[20].

3 RESULTS AND ANALYSIS

3.1 Two main exothermic transformation during devitrification of $Al_{87}Ni_7Cu_3Nd_3$ metallic glass under continuous heating regime

Fig. 1 shows the DSC curve of the $Al_{87}Ni_7Cu_3Nd_3$ amorphous alloy under continuous heating regime at a heating rate of 40 ℃/min. Two main exothermic peaks are observed on the curve, which correspond to two main devitrifying stages[13-16]. X-ray diffraction patterns in Fig. 2 indicates that, the first broad and asymmetric peak corresponds to primary crystallization of the amorphous phase to precipitate Al crystal particles, and the second sharp one corresponds to further transformation of the residual amorphous phase into a multi-phase mixture of Al crystal plus some intermetallic compounds, mainly Al_3Ni, Al_8Cu_4Nd and $Al_{11}Nd_3$. The second DSC peak consists of two overlapped sub-peaks. It is indicated that two reactions that are not completely separated occur in the residual amorphous phase during secondary crystallization.

3.2 HRTEM structural characterization of $Al_{87}Ni_7Cu_3Nd_3$ metallic glass during primary crystallization under continuous heating regime

XRD pattern of the as-prepared samples, as seen in Fig. 2, shows typical amorphous mound. No appreciable crystalline peaks appear. This result is confirmed further by HRTEM and SAED, as shown in Fig. 3(a). Maze contrast of HRTEM image and diffuse halo of SAED pattern suggest that the as-quenched $Al_{87}Ni_7Cu_3Nd_3$ ribbon mainly consists of a fully and homogeneously amorphous phase. However, it is worth noting that, some areas in the as-spun samples show high density of quenched-in nuclei, or cluster and even a few Al crystal of ≤5 nm in diameter, as shown clearly in Fig. 3(b). Hence, the as-quenched ribbon exhibits a uniform amorphous microstructure but with nanoscale compositional or structural heterogeneity.

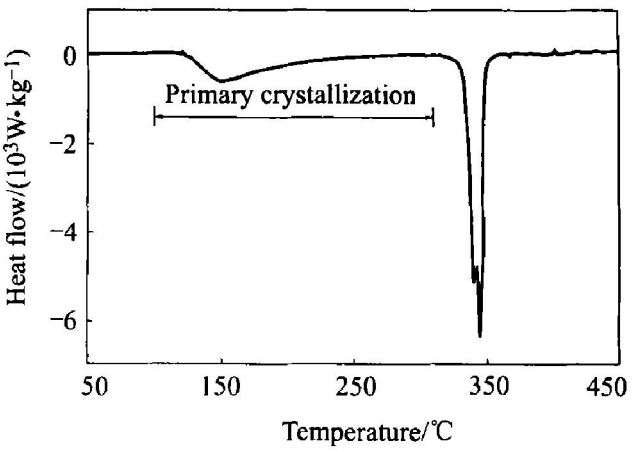

Fig. 1 DSC curve of $Al_{87}Ni_7Cu_3Nd_3$ amorphous alloy under continuous heating regime at heating rate of 40 ℃/min

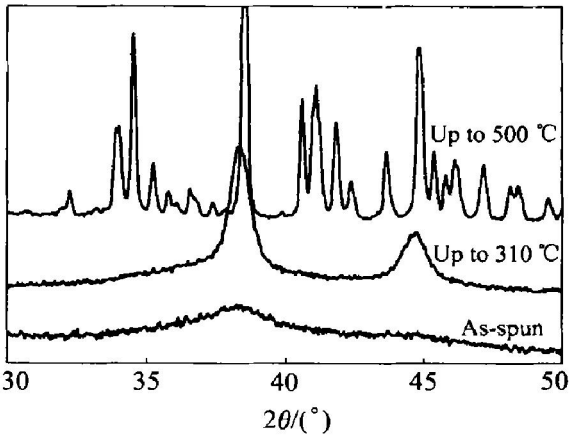

Fig. 2 Typical XRD patterns of as-spun ribbon and its annealed samples heated continuously to various temperatures at heating rate of 40 ℃/min

When heated continuously at 40 ℃/min, the α-Al crystal nuclei form, multiply and grow rapidly in the as-spun $Al_{87}Ni_7Cu_3Nd_3$ metallic glass. With increasing temperature, the annealed ribbons develop gradually into typical primary crystallized morphologies, as shown in Fig. 4. In the sample heated up to 310 ℃, very close to onset temperature of the second DSC peak, high dense α-Al crystalline particles, 5 - 15 nm in diameter, embed dispersively in the amorphous matrix with random orientation. The five diffusion rings in the inset of Fig. 4 correspond to Al (111), (200), (220), (311), and (222) planes, respectively. About 60% (volume fraction) of amorphous phase still remains in the annealed ribbon, by which the α-Al

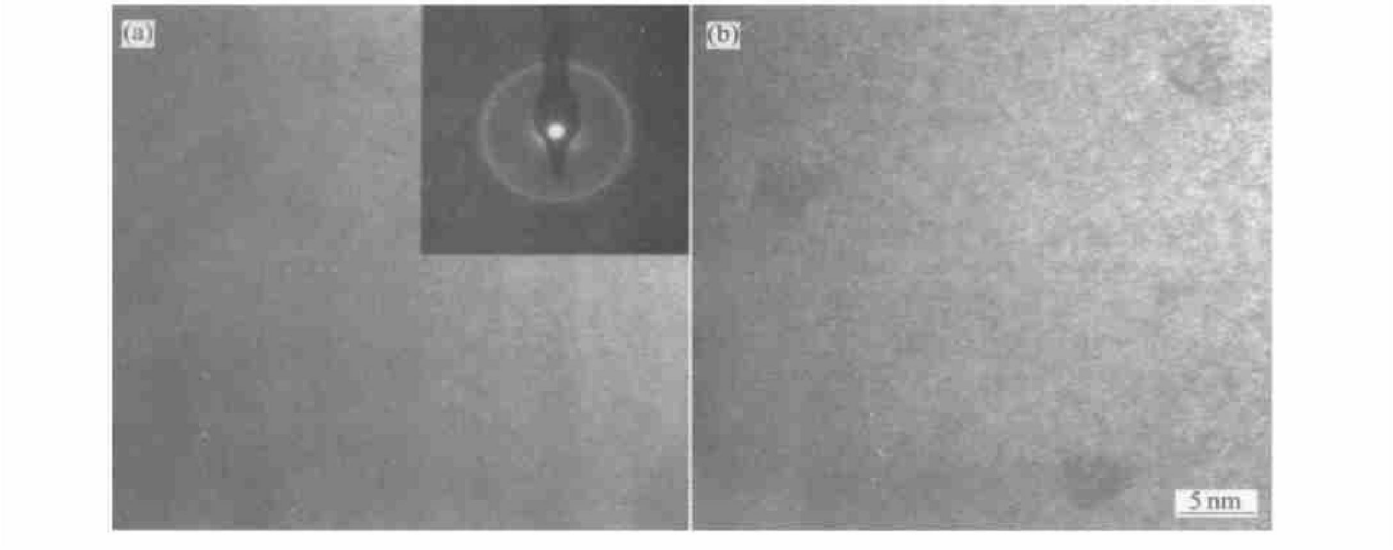

Fig. 3 Bright field HRTEM micrographs and SAED pattern from as-quenched $Al_{87}Ni_7Cu_3Nd_3$ ribbon, showing fully amorphous structure, but with highly dense quenched-in clusters and even a few crystallite embryos in some regions

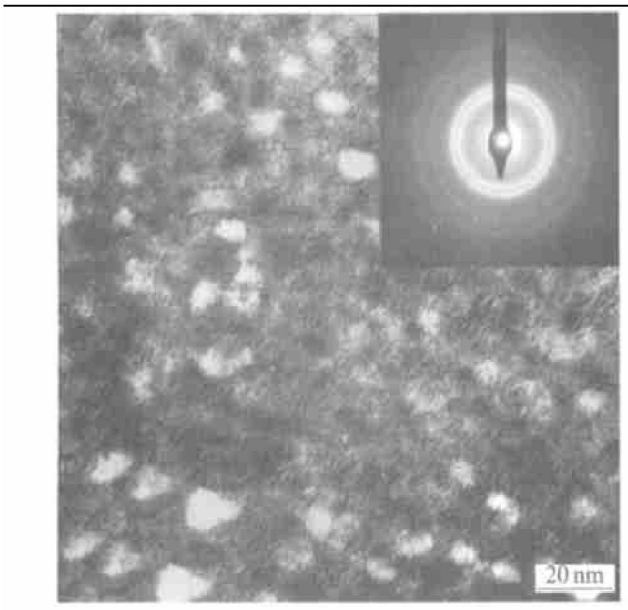

Fig. 4 Bright field HRTEM micrographs and SAED pattern from annealed ribbon heated continuously up to 310 ℃

particles were separated with each other.

Hence, primary crystallization below onset temperature of the second DSC peak results in forming two-phase mixture of the α-Al crystal plus the Ni, Nd and Cu-enriched residual amorphous phase in the rapidly solidified $Al_{87}Ni_7Cu_3Nd_3$ metallic glass.

3.3 Change of volume fraction and mean diameter of primary crystallized Al particles calculated by fitting of X-ray diffraction patterns with heating temperature

Assuming that the annealed ribbons consist of only two phases of the remained amorphous phase and the Al particles after primary crystallization, volume fraction F_{cryst} of primary crystallized Al particles in the two-phase mixture is measured by fitting their corresponding XRD spectra through the following relationship,

$$I = (1 - F_{cryst}) \times I_{amorph} + F_{cryst} \times I_{cryst} \quad (1)$$

where I is the intensity of experimental XRD spectra from the measured sample, I_{amorph}, from the full amorphous ribbon, and I_{cryst}, from pure nanocrystalline phase. The XRD spectra from pure nanocrystal with different grain radii are calculated by using the Debye equation[25-28].

$$I(q) = \sum_i \sum_j f_i(q) f_j(q) (\sin(qr_{ij})/(qr_{ij})) \quad (2)$$

where $I(q)$ is angle-dependent intensity from coherent scattering, sums over i and j are over all the atoms, r_{ij} is the distance between atom i and j, the f's are angle-dependent atomic scattering factors, and $q = 4\pi\sin(\theta)/\lambda$ Here, the following discrete form of the Debye equation is used to fit the intensity of the experimental XRD spectra[26-28],

$$I(S) = I_0 \frac{f^2(S)}{2\pi S} \sum_k \frac{p(r_k)}{r_k} \sin(2\pi r_k S) \quad (3)$$

where $I(S)$ is the diffraction intensity, I_0 is the incident intensity, $f(S)$ is the scattering factor, S is the scattering parameter ($S = q/2\pi$), and r_k and $p(r_k)$ are inter-atomic distance and number of times that a given inter-atomic distance r_k occurs.

This fitting method can also give us mean size d_{cryst} of Al nanocrystal particles in the amorphous matrix, which equals the grain size of pure nanocrystal selected to fit best the experimental XRD spectra. Fig. 5 shows the fitting results of the experimental and calculated XRD spectra, and they are in good agreement with each other. It is indicated that the

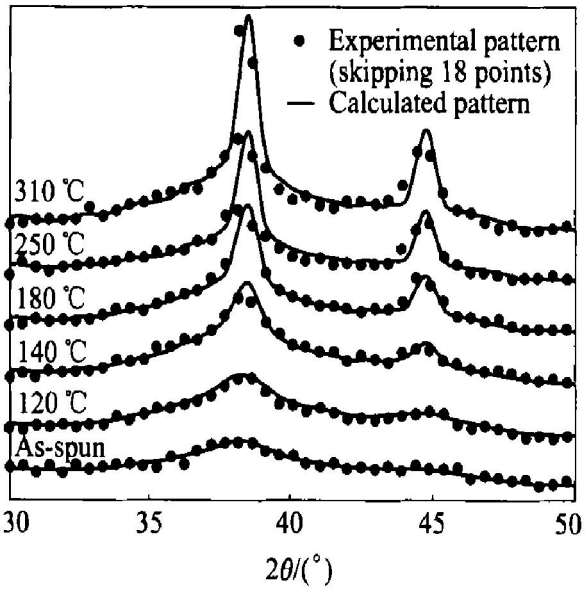

Fig. 5 X-ray diffraction patterns from as-quenched $Al_{87}Ni_7Cu_3Nd_3$ ribbon and specimens heated continuously up to different low temperatures and their respectively calculated patterns

mean size d_{cryst} of the pure nanocrystal selected during calculation is very close to that of the Al crystal particles in the annealed sample, respectively.

The calculated F_{cryst} and the selected d_{cryst} are summarized in Fig. 6, which shows the change of mean diameter and volume fraction of α-Al crystal in the amorphous matrix of the annealed ribbons with heating temperature when continuously heated at 40 ℃/min. Generally, both the volume fraction and the mean diameter of α-Al crystalline particles embedded in the amorphous matrix increase with temperature, as seen in Figs. 6(a) and 6(b), respectively. At lower temperature the α-Al crystal particles grow at a larger rate, and the relative amount of phase transformation also increases more rapidly, and when heated up to higher temperature both the mean diameter and the volume fraction change at a lower rate due to being limited by build-up and overlapped diffusion field of Ni and Nd solute atoms with low diffusion rate, and gradually get close to some stable values, 13 - 15 nm and 30% - 40%, respectively.

Obviously, the α-Al crystal particles become very large within short time due to rapid devitrification at high temperature, and even accompanied by a very small amount of orthorhombic Al_3Ni intermetallic compounds at 310 ℃, which has been verified by HRTEM. Hence, it is difficult to control structural evolution by using high temperature annealing and to yield novel nanophase composites with ideal nanostructure. Therefore, low temperature annealing treatment below 160 ℃ is more beneficial to obtaining the nanophase composites with excellent combination of mechanical properties.

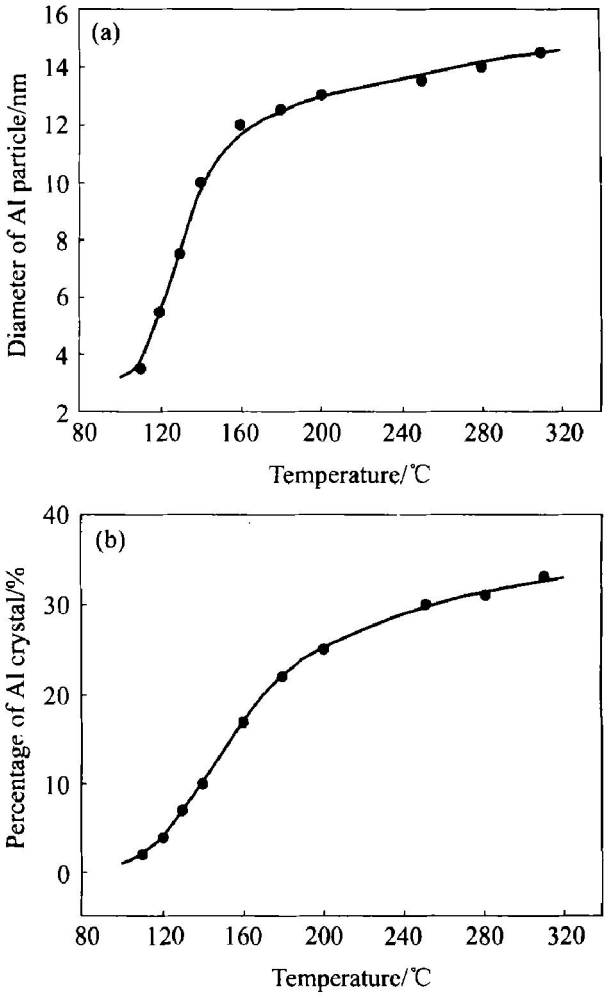

Fig. 6 Mean diameter (a) and volume fraction (b) of α-Al crystal in amorphous matrix of $Al_{87}Ni_7Cu_3Nd_3$ metallic glass versus heating temperature at 40 ℃/min

4 CONCLUSIONS

1) The as-spun $Al_{87}Ni_7Cu_3Nd_3$ ribbon consists of a homogeneous and fully amorphous structure on the micron scale, but with high density of nanoscale quenched-in clusters or crystallite embryos. Primary crystallization mainly leads to formation of two-phase mixture, consisting of large amount of α-Al nanocrystal particles dispersed uniformly in the residual amorphous matrix.

2) To fit the XRD spectra of the two-phase mixture by using the Debye equation, the calculated spectra have good agreement with the experimental spectra, and the calculated values of α-Al nanocrystal volume fraction and mean diameter can characterize the primary crystallization process of the fully amorphous phase very well.

3) Both the volume fraction and mean diameter of α-Al crystalline particles increase more rapidly at the earlier stage (lower temperature) than at the later stage (higher temperature) of primary crystallization due to being limited by build-up and overlapped diffusion field of Ni and Nd solute atoms with low diffu-

sion rate. With increasing transformation temperature, they will gradually get close to some saturated value, 13 – 15 nm and 30% – 40%, respectively.

ACKNOWLEDGEMENTS

This work was carried out in Universidad de Barcelona (UB) and Universidad Autonomo de Barcelona (UAB). Dr. XIAO thanks the Agencia Española de Cooperacion International (AECI) and the China Scholarship council (CSC) for providing an international scholarship for studying in Spain.

The financial supports from the Comission Interministerial de Ciencia y Tecnologia (CICYT) by Project No. MAT92-0501, Project No. MAT96-00692, and Project No. MAT98-00672, and from the Comission Interdepartemental de Ciencia I Tecnologia (CIRIT) by Project 1999SGR-00336, and the help given by the Seiveis Cientifico-Tecnics of The Universidad de Barcelona in the HRTEM and HTXRD, are acknowledged.

REFERENCES

[1] He Y, Poon S J, Shifet G J. Synthesis and properties of metallic glasses that contain aluminum [J]. Science, 1988, 241: 1640 – 1642.

[2] Inoue A, Ohtera K, Kita K, et al. New amorphous alloys with good ductility in Al-Ce-M (M = Nb, Fe, Co, Ni or Cu) systems [J]. Jpn J Appl Phys, 1988, 27 (8): 1796 – 1799.

[3] Inoue A, Ohtera K, Tsai A P, et al. Glass transition behavior of Al-Y-Ni and Al-Ce-Ni amorphous alloys [J]. Jpn J Appl Phys, 1988, 27 (3): 280 – 282.

[4] Wu R I, Wilde G, Perepezko J H. Glass formation and primary nanocrystallization in Al-base metallic glasses [J]. Mater Sci Eng, 2001, A301(1): 12 – 23.

[5] Kim Y H, Soh J R, Kim D K, et al. Glass formation in metallic Al-Ni-Y [J]. J Non-Crystalline Solids, 1998, 242 (2 – 3): 122 – 130.

[6] Yewordwossen M, Dunlap R A, Lloyd D J. Thermal and electronic properties of $Al_{87}Y_8Ni_{5-x}TM_x$ (TM = Mn, Fe, Co, Cu.) [J]. J Phy: Condens Mater, 1992, (4): 461 – 472.

[7] Das S K, Perepezko J H, Wu R I, et al. Undercooling and glass formation in Al-based alloys [J]. Mater Sci Eng, 2001, A304 – 306 (1): 159 – 168.

[8] Gich M, Gloriant T, Surinñach S, et al. Glass forming ability and crystallization processes within Al-Ni-Sm system [J]. Journal of Non-Crystalline Solids, 2001, 289 (2): 214 – 220.

[9] Greer A L. Metallic glasses [J]. Science, 1995, 267: 1947 – 1953.

[10] Greer A L. Crystallization of amorphous alloys [J]. Metall Mater Trans, 1996, 27 (3): 549 – 556.

[11] Allen D R, Foley J C, Perepezko J H. Nanocrystal development during primary crystallization of amorphous alloys [J]. Acta Metall Mater, 1998, 46 (2): 431 – 440.

[12] Tsai A A, Kamiyama K, Kawamura Y, et al. Formation and precipitation mechanism of nanoscale Al particles in Al-Ni based amorphous alloy [J]. Acta Mater, 1997, 45 (4): 1477 – 1487.

[13] Clavaguera-Mora M T. The use of metastable phase diagrams in primary crystallization kinetics study [J]. Thermochimica Acta, 1998, 314 (1 – 2): 281 – 289.

[14] Clavaguera N, Diego J A, Clavaguera-Mora M T, et al. Nanocrystalline formation of AlNiNdCu materials: a kinetic study [J]. Nanostructured Materials, 1995, 5 (6): 485 – 488.

[15] Clavaguera-Mora M T, Rodriguez-Viejo J, Jacovkis D, et al. Neutron diffraction and calorimetric studies on Al-based metallic glasses [J]. J Non-Cryst Solids, 1998, 287 (1): 162 – 169.

[16] Clavaguera N, Clavaguera-Mora M T. Supercooled liquid properties versus glass formation: Application to Al-rich alloys [J]. Scandinavian Journal of Metallurgy, 2001, 30(1): 1 – 8.

[17] Inoue A. Amorphous, nanoquasicrystalline and nanocrystalline alloys in Al-based systems [J]. Prog Mater Sci, 1998, 43 (3): 365 – 532.

[18] Inoue A, Kimura H. Fabrications and mechanical properties of bulk amorphous, nanocrystalline, nanoquasicrystalline alloys in aluminum-based system [J]. Journal of Light Metals, 2001, 10(1): 31 – 41.

[19] Kim Y H, Inoue A, Masumoto T. Increase in mechanical strength of Al-Y-Ni amorphous alloy by dispersion of nanoscale fcc-Al particle [J]. Mater Trans JIM, 1991, 32(4): 381 – 338.

[20] Kim Y H, Inoue A, Masumoto T. Ultrahigh tensile strength of $Al_{88}Y_2Ni_9M_1$ (M = Mn or Fe) amorphous alloys containing finely dispersed FCC Al particles [J]. Mater Trans JIM, 1990, 31: 747 – 749.

[21] Shiflet G J, He Y, Poon S J. Mechanical properties of a new class of metallic glasses based on aluminum [J]. J Appl Phys, 1988, 64(12): 6863 – 6865.

[22] Jiang X Y, Zhang Z C, Greer A L. Particle-size effects in primary crystallization of amorphous Al-Ni-Y alloys [J]. Mater Sci Eng, 1997, A226-228: 789 – 793.

[23] Zhang Z C, Jiang X Y, Greer A L. Microstructure and hardening of Al-based nanophase composites [J]. Mater Sci Eng, A226 – 228: 531 – 536.

[24] Foley J C, Allen D R, Perepezko J H. Strategies for the development of nanocrystalline materials through devitrification [J]. Mater Sci Eng, 1997, A226 – 228: 569 – 573.

[25] Warren B E. X-Ray Diffraction [M]. New York: Dover Publications, INC, 1990. 250 – 261.

[26] Bawendi M G, Kortan A R, Steigerwald M L, et al. Investigation on CdSe films prepared by chemical deposition by X-ray diffraction [J]. J Chem Phy, 1989, 91 (11): 7282 – 7293.

[27] Hall B D, Monot R. Calculating the Debye-Scherrer diffraction pattern for large clusters [J]. Computer in Physics, 1991, (3): 414 – 426.

[28] Trojanek F, Cingolani R, Cannoletta D. Tailoring of nanocrystal sizes in CdSe films prepared by chemical deposition [J]. Journal of Crystal Growth, 2000, 209 (4): 695 – 700.

(Edited by PENG Chao-qun)